

Pionic decay of Λ hypernuclei

J. Nieves and E. Oset

*Departamento de Física Teórica and Instituto de Física Corpuscular, Centro Mixto,
Universidad de Valencia–Consejo Superior de Investigaciones Científicas, 46100 Burjassot, Valencia, Spain*
(Received 23 March 1992)

We evaluate pionic decay widths of Λ hypernuclei using shell-model nuclear wave functions and distorted pion waves. We investigate the effects of the final-state interaction of the pion, consider decay into nuclear bound states and the continuum for the nucleons, and make an accurate study of the energy balance in the reaction. The results obtained confirm many previous findings but also modify appreciably previous results, mostly as a consequence of the accurate treatment of the energies involved in the reaction.

PACS number(s): 21.80.+a, 23.90.+w

I. INTRODUCTION

The mesonic decay of Λ hypernuclei has received attention in the past with most measurements done in emulsion experiments [1], although some direct measurements are now being performed [2–5]. At the same time the subject has also received theoretical attention, in both light nuclei [6–8] and medium and heavy nuclei [9–13]. One of the peculiar features of the mesonic Λ decay is that the Pauli blocking produces a substantial reduction of the decay width with respect to its free value. On the other hand, another interesting feature of this process is that it is very sensitive to the pion nuclear wave function in the medium. This was first shown in Ref. [10], where the renormalization of the pion in the medium led to large enhancements of the mesonic width. More detailed work by following an alternative method sketched in Ref. [14] is done in Refs. [11–13]. A thorough work over the periodic table is done in the latter references and the sensitivity to the pion nucleus optical potential is manifestly shown. A review of experimental and theoretical work can be found in Refs. [15,16].

In the present work we follow the same method as in Refs. [11–13] and perform a detailed study of the mesonic decay in several nuclei over the periodic table. The novelties which we introduce are the following.

(i) We use an optical potential which has been deduced theoretically and to which some small pieces (of the order of 15% of the calculated part) are added in order to fit the data of pionic atoms. With this potential one obtains a good reproduction of the pionic atom data [17] and low-energy pion nucleus scattering [18]. One of the advantages of this potential is that it allows the separation of the imaginary part into a piece related to the quasielastic reaction channel and another one related to pion absorption, the two reaction channels in the scattering of pions before pion production sets in at higher energies. This separation is useful since it allows one to evaluate the quasielastic and absorption cross sections as a function of the pion energy. The results obtained in Ref. [18] for these cross sections and for the differential elastic cross sections agree fairly well with experiment.

This separation is of relevance for the present problem. Indeed, the method followed in Refs. [11–13] uses a full optical potential to distort the pions. The effect of the imaginary part of the potential is to remove from the emerging pion flux those pions which undergo quasielastic scattering or pion absorption. However, while the pions absorbed should be definitely removed, this is not the case with those which undergo quasielastic scattering, since even if they collide, they are still there and will be observed. This means that one should not remove these pions from the pion flux and we take this into account here.

(ii) In Ref. [11] it was shown that in medium and heavy nuclei most of the strength in the mesonic decay goes to nucleons from $\Lambda \rightarrow N\pi$ populating excited nuclear bound states. The continuum is implicitly considered by summing over discrete states of the harmonic oscillator until convergence is found. There are two approximations in this procedure: On the one hand, the wave functions of the nucleons in the continuum are replaced by those of the harmonic oscillator, on the other hand, the set of continuum energies is replaced by discrete levels separated by $\hbar\omega$. In the present paper we have made a more realistic evaluation of the strength in the continuum.

(iii) The precise determination of the energy of the emerging pions is very important. Smaller momenta of the pion reduce the width for two reasons: the Pauli blocking is more effective and the p -wave attraction (roughly proportional to q^2) is also reduced and this weakens the enhancement produced by the renormalization of the pion waves. Hence, a small change in the pion momentum leads to appreciable changes in the mesonic width. For this reason we have taken care of the energy balance rather accurately by relying upon the experimental energies of the nuclei involved in the process. This latter effect modifies the results appreciably with respect to those of Refs. [11–13] where the energies are obtained from the shell model, although some phenomenological information is also used. This also leads to results for the π^0 and π^- decay which are rather different from what we might expect from the use of the same shell model for protons and neutrons.

The widths obtained, measured in units of the free width, range from about 10^{-1} to 10^{-4} from medium to heavy nuclei for decay in π^-p , or 10^{-1} – 10^{-5} for decay in π^0n .

II. THE MESONIC Λ WIDTH

We start from a Lagrangian for $\Lambda \rightarrow \pi N$ decay

$$L_{\pi N \Lambda} = G\mu^2 \bar{\psi}_N (A - B\gamma_5) \boldsymbol{\tau} \cdot \boldsymbol{\phi}_\pi \psi_\Lambda + \text{H.c.}, \quad (1)$$

where the terms A and B correspond to the parity-violating and parity-conserving parts of the interaction, respectively. By following Ref. [19], ψ_Λ is assumed to behave as the neutron state of an isospin doublet and this implements the $\Delta T = \frac{1}{2}$ rule by means of which the rate of $\Lambda \rightarrow \pi^- p$ is twice as large as that of $\Lambda \rightarrow \pi^0 n$. Equation (1) leads to an operator in nonrelativistic form of the type

$$\delta \bar{H}_{\Lambda \pi N} = -G\mu^2 [S - (P/\mu)\boldsymbol{\sigma} \cdot \mathbf{q}] \tau^\lambda, \quad (2)$$

where

$$\Gamma^{(\alpha)} = \frac{1}{2} C^{(\alpha)} \sum_{N \neq F} \int \frac{d^3 q}{(2\pi)^3} \frac{1}{2\omega(q)} 2\pi \delta(E_\Lambda - \omega(q) - E_N) (G\mu^2)^2 \times \left[S^2 \left| \int d^3 x \varphi_\Lambda(\mathbf{x}) \bar{\varphi}_\pi^{(-)}(\mathbf{q}, \mathbf{x})^* \varphi_N^*(\mathbf{x}) \right|^2 + \left[\frac{P}{\mu} \right]^2 \left| \int d^3 x \varphi_\Lambda(\mathbf{x}) \nabla \bar{\varphi}_\pi^{(-)}(\mathbf{q}, \mathbf{x})^* \varphi_N^*(\mathbf{x}) \right|^2 \right], \quad (5)$$

where $\varphi_N, \varphi_\Lambda$ are the nucleon and lambda wave functions, E_N and E_Λ their corresponding energies, $\omega(q)$ the pion energy, and the sum over N runs over the unoccupied orbitals n, l since spin sums are already performed. We hence do not consider the spin-orbit splitting of the levels and work in an l, s basis for the nuclear excited states. In Eq. (5) and what follows the sums over N are over proton or neutron orbitals according to α .

The pion wave function $[\bar{\varphi}_\pi^{(-)}(\mathbf{q}, \mathbf{x})^*]$ as a block corresponds to an incoming solution of the Klein-Gordon equation:

$$[-\nabla^2 + \mu^2 + 2\omega V_{\text{opt}}(\mathbf{x})] \bar{\varphi}_\pi^{(-)}(\mathbf{q}, \mathbf{x})^* = [\omega - V_C(\mathbf{x})]^2 \bar{\varphi}_\pi^{(-)}(\mathbf{q}, \mathbf{x})^*, \quad (6)$$

$$\Gamma^{(\alpha)} = C^{(\alpha)} (G\mu^2)^2 \frac{1}{4\pi} \sum_{j=n, l \neq F} q_j \frac{1}{1 + \omega(q_j)/M_A} \left[S^2 S_j^{(s)}(q_j) + \left[\frac{P}{\mu} \right]^2 q_j^2 S_j^{(p)}(q_j) \right], \quad (8)$$

$$q_j = [(E_\Lambda - E_j)^2 - \mu^2]^{1/2}, \quad (9)$$

where E_j is the energy of the nucleon in the level n, l . We have implemented the recoil factor $(1 + \omega/M_A)^{-1}$ because according to Ref. [11], and as we shall see, most of the decay corresponds to nucleons in nuclear bound excited states and as a consequence the nucleus recoils as a whole. $S_\pi^{(s)}(q_j)$ and $S_\pi^{(p)}(q_j)$ are the s - and p -wave suppression factors

$$(G\mu^2)^2 / 8\pi = 1.945 \times 10^{-15},$$

$$S \equiv A = 1.06, \quad (3)$$

$$P \equiv B\mu/2M = 0.527,$$

and μ and M are the pion and nucleon mass, respectively.

The free width is readily evaluated and leads for proton or neutron decay to

$$\Gamma_{\text{free}}^{(\alpha)} = C^{(\alpha)} (G\mu^2)^2 \frac{1}{4\pi} \frac{M q_{\text{c.m.}}}{M_\Lambda} \left[S^2 + \left[\frac{P}{\mu} \right]^2 q_{\text{c.m.}}^2 \right], \quad (4)$$

$$q_{\text{c.m.}} = \frac{\lambda^{1/2}(M_\Lambda^2, M^2, \mu^2)}{2M_\Lambda}, \quad C^{(p)} = 4, \quad C^{(n)} = 2,$$

with M_Λ the Λ mass and $q_{\text{c.m.}}$ the pion momentum in the center-of-mass frame. One can see from Eq. (4) that the parity-violating term is the dominant one in the decay.

The width for the Λ decay inside a nucleus is given by

with $V_C(\mathbf{x})$ the Coulomb potential created by the nucleus considering finite size effects. One can see that [20]

$$\bar{\varphi}_\pi^{(-)}(\mathbf{q}, \mathbf{x})^* \equiv \varphi_\pi^{(+)}(-\mathbf{q}, \mathbf{x}), \quad (7)$$

where $\varphi_\pi^{(+)}(-\mathbf{q}, \mathbf{x})$ corresponds to an incoming solution for a pion of momentum $-\mathbf{q}$.

The use of Eq. (7) for the outgoing pion wave function guarantees that pion flux is lost to the reaction channels (accounted for by the imaginary part of the complex optical potential), when the pions move out through the nucleus.

By performing the \mathbf{q} integral in Eq. (5) we obtain for closed-shell nuclei

$$S_j^{(s)}(q) = \left| \int d^3 x \varphi_\Lambda(\mathbf{x}) \varphi_\pi^{(+)}(-\mathbf{q}_j, \mathbf{x}) \varphi_j^*(\mathbf{x}) \right|^2, \quad (10)$$

$$S_j^{(p)} = \frac{1}{q_j^2} \left| \int d^3 x \varphi_\Lambda(\mathbf{x}) [\nabla \varphi_\pi^{(+)}(-\mathbf{q}_j, \mathbf{x})] \varphi_j^*(\mathbf{x}) \right|^2.$$

A little bit of algebra allows one to write

$$\begin{aligned}
S_j^{(s)} &= (2l+1) |I_{nl}(q_j)|^2, \\
S_j^{(p)} &= \frac{1}{q_j^2} [l |M_{nl}(q_j)|^2 + (l+1) |N_{nl}(q_j)|^2], \\
I_{nl}(q) &= \int_0^\infty r^2 dr R_{1s}^{(\Lambda)}(r) \tilde{j}_l(q_j; r) R_{nl}(r), \\
M_{nl}(q_j) &= \int_0^\infty r^2 dr R_{1s}^{(\Lambda)}(r) \left[\frac{d\tilde{j}_{l-1}(q_j; r)}{dr} - (l-1) \frac{\tilde{j}_{l-1}(q_j; r)}{r} \right] R_{nl}(r), \\
N_{nl}(q_j) &= \int_0^\infty r^2 dr R_{1s}^{(\Lambda)}(r) \left[\frac{d\tilde{j}_{l+1}(q_j; r)}{dr} + (l+2) \frac{\tilde{j}_{l+1}(q_j; r)}{r} \right] R_{nl}(r),
\end{aligned} \tag{11}$$

where $\tilde{j}_l(q_j; r)$ are the radial wave functions of the pion for each partial wave, regular in the origin and with the boundary conditions

$$\tilde{j}_l(q; r)_{r \rightarrow \infty} \simeq \begin{cases} e^{i\delta_l} \frac{1}{qr} \sin \left[qr - l\frac{\pi}{2} + \delta_l \right] & \text{for } \pi^0 \\ e^{i(\delta_l + \sigma_l)} \frac{1}{qr} \sin \left[qr - l\frac{\pi}{2} + \sigma_l + \delta_l - \eta \ln 2qr \right] & \text{for } \pi^- , \end{cases} \tag{12}$$

with η and σ_l defined as in Ref. [20] and δ_l the complex phase shifts obtained from the numerical solution of the Klein-Gordon equation. Since $\text{Im } \delta_l > 0$, we obtain a damping of all the matrix elements due to the imaginary part of the pion optical potential.

Equations (11) agree with those of Ref. [11] but are somewhat simpler. A generalization for nonclosed shells accounting for spin-orbit splitting is done in Ref. [12]. In the absence of distortion on the pion waves, $\tilde{j}_l(q; r)$ becomes the ordinary Bessel function, $j_l(qr)$, and $S_j^{(s)} = S_j^{(p)}$.

III. LAMBDA AND NUCLEON WAVE FUNCTIONS

For medium and heavy hypernuclei the shell model for the Λ particles works remarkably well [21–23]. We have thus taken a potential (in MeV) [23]

$$V(r) = -32\rho(r)/\rho_0, \tag{13}$$

where $\rho(r)$ is the nuclear density and $\rho_0 \equiv \rho(r=0)$.

This potential reproduces fairly well the Λ levels. With this potential we evaluate numerically the Λ wave function for the ground state as well as its binding energy. The values obtained for the Λ binding are shown in Table I for the different nuclei used in the present work.

TABLE I. Λ binding energies (B_Λ) for the different nuclei used in this work. T_π^b is the π (π^- or π^0) kinetic energy when the nucleon, which comes from the Λ decay, goes to the first free level of the nucleus A (ground state of the $A+1$ nucleus).

Nucleus ($A + \Lambda$)	B_Λ (MeV)	T_π^b (MeV)	$T_{\pi^0}^b$ (MeV)
$^{12}_\Lambda\text{C}$	12.4	26.0	47.4
$^{17}_\Lambda\text{O}$	13.1	25.2	32.1
$^{41}_\Lambda\text{Ca}$	19.7	19.2	29.8
$^{91}_\Lambda\text{Zr}$	25.0	17.9	23.2
$^{139}_\Lambda\text{Ba}$	26.8	17.2	19.1
$^{209}_\Lambda\text{Pb}$	28.0	13.4	16.8

For the nucleons we have used the following potential (in MeV) [24]:

$$V(r) = -50f(r),$$

where

$$f(r) = \frac{1}{1 + \exp[(r-R)/a]}, \tag{14}$$

with $R = 1.25 A^{1/3}$ fm, $a = 0.65$ fm, which provides a fair reproduction of the nuclear levels for the average energy of major shells, as well as realistic nucleon wave functions. However, since the energy balance in this reaction is so important we have relied upon experimental values of the energy of the nuclei involved rather than on the absolute values provided by the shell model. In this way we take into account corrections to this shell model from isospin or Coulomb effects as well as differences coming from the complexity of the interaction of the many-body system. Thus, the absolute value of the nuclear energies in the transition from the ground state of the (A) system to the ground state of the ($A+1$) system are taken from the experimental value of the masses of the A and ($A+1$) nuclear states. Then, the shell model provides the energy of the excited states, once the origin has been set by the experiment, plus the wave functions for all the nucleon states.

As an example let us take $^{209}_\Lambda\text{Pb} \rightarrow ^{209}\text{Pb } \pi^0$ and $^{209}_\Lambda\text{Pb} \rightarrow ^{209}\text{Bi } \pi^-$. In the first case we have

$$M(^{209}\text{Pb}) - M(^{208}\text{Pb}) = 935.7 \text{ MeV}, \tag{15}$$

where the masses indicate the masses of the neutral atoms following Ref. [25]. In Eq. (15) the difference also holds for the difference of the nuclear masses which we need here.

In the shell model the first level where the neutron can go in the ^{209}Pb nucleus is the $1i$ orbital, which has binding energy of -9.6 MeV. Hence

$$m_n + E(1i) = 930.0 \text{ MeV} . \quad (16)$$

Thus the shell model underestimates the experimental energy by 5.7 MeV. Conversely, we can say that the pion would go out with 5.7 MeV less than what the shell model provides. Hence this is what we do in practice: we subtract this energy from the pion by effectively assuming that the Λ energy is reduced in that amount. For the π^- decay we have ^{208}Pb

$$M(^{209}\text{Bi}) - M(^{208}\text{Pb}) = 935 \text{ MeV} \quad (17)$$

and the difference between the nuclear masses is 935 MeV $- m_e$, with m_e the electron mass. The first level where the proton can go in ^{109}Bi is the $1h$ orbit which has binding energy of -17.2 MeV. Hence the shell-model value

$$m_p + E(1h) = 921.1 \text{ MeV} \quad (18)$$

undercounts the experimental energy in 13.4 MeV.

We have written in Table II the experimental values of $M(A+1) - M(A)$. In this table, we have also shown the difference Δ between $m_N + E_0$ (E_0 is the energy of the first level populated by the nucleon, which comes from the Λ decay, in the $A+1$ system) and $M(A+1) - M(A)$ (plus the electron mass in the case of $\pi^- p$ decay). This magnitude has to be added to the pion energy with respect to the results provided by the shell model. Accordingly, one obtains the values for the pion energy in the ground-state-to-ground-state transitions which are shown in Table I.

In Ref. [11] shell-model energies are considered and Coulomb corrections added. However, the procedure does not provide appropriate Q values for the reactions. This can be seen by looking at the maximum value of the π^0 and π^- momenta quoted in Ref. [11] for different nuclei and contrasting the differences between the π^0 and

π^- energies with the differences between the masses of the isotopes involved in the reaction. Consideration of this energy balance is important. For instance, in ^{209}Pb the π^- comes with about 13 MeV less energy than what is provided by the shell model and the π^0 with roughly 6 MeV less.

In order to take into account the states in the continuum we discretize them in the following way [26]. We replace the potential of Eq. (14) by the same one but with an infinite barrier at $r=R$. R is chosen such that the modification in the wave function of the bound states and their energies, with respect to the results with the potential without the barrier, are negligible. On the other hand, we also demand that the spacing of the states which appear now at positive energies is small compared with the typical energies which the pion carries. For instance, this is achieved by choosing $R=20$ fm, in the case of ^{208}Pb . The procedure is obviously exact in the limit of $R=\infty$. In particular, increasing R beyond 20 fm does not significantly alter the results for this part of the spectrum which is only a small fraction of the total.

Some of the nuclei which we use are not closed-shell nuclei in the l,s coupling. In this case the nucleons from the Λ decay can fill up n_h empty states in an n,l shell (counting spin). We take that into account by multiplying $S_j^{(s)}$ and $S_j^{(p)}$ from Eqs. (11) by $n_h/2(2l+1)$.

Considering the spin-orbit splitting as in Ref. [12] leads to the same result for $S_j^{(s)}$ and somewhat modified for $S_j^{(p)}$. For light and medium nuclei, where $S_j^{(s)}$ largely dominates the decay, our procedure leads then to basically the same results as if the spin orbit is considered. For heavy nuclei $S_j^{(p)}$ is much more strongly enhanced by the pion renormalization than $S_j^{(s)}$, as shown in Refs. [11–13] and confirmed here, and hence the p -wave part contributes more to the width in these nuclei. However, we shall see that the p -wave part contribution is still a fraction of the s -wave contribution, and hence the neglect of the spin-orbit splitting has no practical consequences. On the other hand, since a large fraction of the width already

TABLE II. First column: Λ hypernucleus ($A+\Lambda$) (Z). Second column: Daughter [$A+1(Z+1)$, $A+1(Z)$] nuclei after Λ decay. Third column: Experimental energy differences between the daughter neutral atoms and the neutral atom associated to the core of the Λ hypernucleus $A(Z)$. Fourth column: Binding energy of the first free level of the nucleus $A(Z)$. Fifth column: Correction which we added to the pion energy as is explained in the text.

$A+\Lambda$	$A+1$	$M(A+1) - M(A)$ (MeV)	First level E_0 (MeV)	Δ (MeV)
$^{12}_{\Lambda}\text{C}$	$\pi^- p$ ^{12}N	938.2	$1p(-9.3)$	-8.7
	$\pi^0 n$ ^{12}C	920.9	$1p(-9.3)$	+9.4
$^{17}_{\Lambda}\text{F}$	$\pi^- p$ ^{17}F	938.2	$2s(-2.1)$	-1.5
	$\pi^0 n$ ^{17}O	935.4	$2s(-2.1)$	+2.1
$^{41}_{\Lambda}\text{Ca}$	$\pi^- p$ ^{41}Sc	937.7	$1f(-3.85)$	-2.7
	$\pi^0 n$ ^{41}Ca	931.2	$1f(-3.85)$	+4.6
$^{91}_{\Lambda}\text{Zr}$	$\pi^- p$ ^{91}Nb	933.6	$1g(-9.1)$	-3.9
	$\pi^0 n$ ^{91}Zr	932.4	$1g(-9.1)$	-1.9
$^{139}_{\Lambda}\text{Ba}$	$\pi^- p$ ^{139}La	932.5	$1g(-17.4)$	-11.1
	$\pi^0 n$ ^{139}Ba	934.8	$1h(-8.85)$	-4.0
$^{209}_{\Lambda}\text{Pb}$	$\pi^- p$ ^{209}Bi	935.0	$1h(-17.2)$	-13.4
	$\pi^0 n$ ^{209}Pb	935.7	$1i(-9.6)$	-5.7

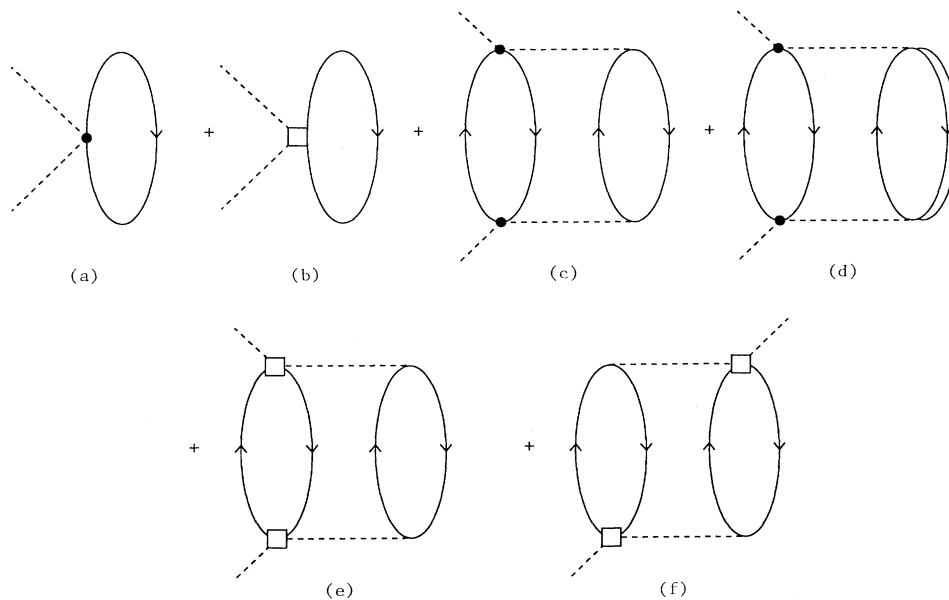


FIG. 1. Diagrammatic representation of the input in the pionic optical potential. The full dot stands for the πN s -wave scattering amplitude; the box for the πN p -wave scattering amplitude. Diagrams (a) and (b) account for the lowest-order optical potential and (c)–(f) for the second-order part: (c) and (d) for the s -wave part and (e) and (f) for the p -wave part.

occurs from the ground-state-to-ground-state transition, considering the proper energy balance as we do here is very important.

IV. THE PION NUCLEUS OPTICAL POTENTIAL

As noted in the introduction the renormalization of the pion wave inside the nucleus is very important and leads to appreciable changes of the mesonic width. We are using here an optical potential which has been developed microscopically and is exposed in detail in Ref. [17] for pionic atoms and in Ref. [18] for scattering problems. Diagrammatically it can be depicted by Fig. 1. It contains the ordinary lowest-order optical potential constructed from the s - and p -wave πN amplitudes plus the second-order terms in the s and p waves depicted there. Standard corrections like the second-order Pauli corrected rescattering term [27], the ATT term [28], and the Lorentz-Lorenz corrections [27] appear in a natural way in the scheme. The pion exchange lines in the figure are replaced by the spin-isospin effective interaction and the ph (particle-hole) or Δh (delta-hole) interaction excited by the pion lines are iterated to all orders to generate the random-phase approximation (RPA) series.

The theoretical potential by itself reproduces the data of pionic atoms within 15%. In order to get a better fit of the data we add a small phenomenological potential which is fitted to the data of pionic atoms and by means of which a better agreement with the data is reached. This latter potential is the one we use here.

Another interesting feature of this potential, of relevance to the present problem, is that it allows to separate the imaginary part from the different sources and relate them to the different channels in the reaction. The imaginary part from a Feynman diagram appears when, in the integration of the variables of the intermediate states, all states cut by a horizontal line in the figure

are placed on shell. At low energies we get such a contribution from Figs. 1(c), 1(e), and 1(f) when the two ph excitations are placed on shell and this corresponds to the channels of pion absorption. However, the quasielastic scattering also contributes to the imaginary part of the potential. This quasielastic contribution is obtained in our model from diagrams like in Fig. 2. Indeed, the imaginary part corresponds there to placing on shell the ph excitation and the pion, which corresponds to the quasielastic channel.

This brief exposition provides a basic idea of what is done in Refs. [17,18] and further details can be seen there. With that potential one gets a good description of the shifts and widths of pionic atoms over the periodic table including the so called anomalous atoms [29] ($3d$ states in heavy nuclei and others). On the other hand, it also provides a good reproduction of the elastic scattering cross sections, as well as the reaction cross section and pion absorption cross section over the periodic table in the range 0–60 MeV. The potential is local for the s -

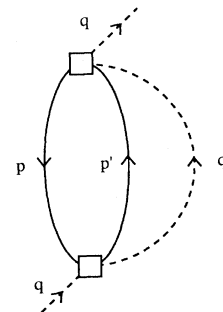


FIG. 2. Rescattering diagram. When the intermediate ph and π lines are placed on shell it provides the quasielastic contribution to the imaginary part of the optical potential.

wave part and contains Kisslinger-like nonlocalities $\nabla f(r)\nabla$ for the p -wave part.

With that potential, and a Coulomb potential for the π^- that accounts for the finite size of the nucleus, we solve numerically the Klein-Gordon equation, Eq. (6) and impose the boundary conditions of Eq. (12) in the radial solutions which are regular in the origin.

V. RESULTS AND DISCUSSION

In order to illustrate the physics of the process we show in detail in Table III the contribution to the mesonic width of $^{209}_{\Lambda}\text{Pb}$ from each of the nuclear levels and the continuum. We show the results for π^-p and π^0n decay using the strict energies which come from the shell model. In the case of π^-p decay the bound levels for the p in ^{209}Bi are $1h, 2f, 3p, 1i, 2g, 3d, 4s, 1j$, while the states $4p, 5s, 3f, 2h, 4d$, etc. appear in the continuum. For π^0n decay the neutron populates the bound states $1i, 2g, 3d, 4s, 1j$ of ^{209}Pb and the same states as before appear in the continuum.

We show there the contribution assuming free pions, this is, considering plane wave for the pions rather than distorted waves, and also the results with distorted pion waves. At the same time we also show the results obtained by switching off the imaginary part of the optical potential related to quasielastic pion scattering in order not to eliminate the pions which undergo quasielastic scattering from the pion flux.

Some striking features appear.

(i) The convergence of the contribution from the different states is rather fast because as the nucleon energy increases the pion momentum decreases and makes the transition from the Λ ground state to the excited nucleon states more difficult [see matrix elements in Eq. (5)]. This was first noticed in Ref. [11]. Some states, particularly those with small angular momentum, have a larger weight because the transition from the Λ $1s$ state is easier.

(ii) The effect of the renormalization of the pion is an enhancement of the π^- decay width by a factor of 60 and of the π^0 width by a factor of 6. This difference between the effect of π^- and π^0 is large and is due to two factors. Indeed, in π^-p decay the p occupies lower orbits than the n from π^0n decay and as consequence the π^- has more energy than the π^0 . Hence, the pionic potential is more attractive in the π^- case since the attractive p -wave part of the potential, which goes roughly as q^2 , has bigger strength. On the other hand, the Coulomb potential also is attractive in the case of the π^- . This attraction leads to larger pion momenta inside the medium which make much easier the transition to the nucleon excited states, thus weakening the effect of Pauli blocking. These features also reconfirm the findings of Refs. [11–13].

(iii) Omitting the quasielastic piece in the imaginary part of the optical potential leads to an enhancement of about 50% in the cross section for π^- decay while it produces only a moderate decrease of 5% in the case of π^0 decay. This different behavior has to be seen in the fact that in the π^- case the quasielastic piece in the imaginary

part of the potential is larger than in the π^0 case since it increases with the pion energy (and vanishes as $q \rightarrow 0$ in the absence of Coulomb forces). When the piece is small, the modifications produced in the pion wave functions and the peculiar matrix elements which one is evaluating can lead to some small reduction, as in the π^0 case here, since one is slightly changing the balance of the large cancellations which occur in these matrix elements.

(iv) The contribution of the continuum is small in the case of the π^- , 0.1%, but larger in the case of the π^0 , 10%. In the absence of distortion this latter fraction is about 50%.

The results discussed above are obtained by using the shell-model energies. In Table IV we show the same results as in Table III, however, taking into account the proper experimental energies, as we discussed in Sec. III. Hence we add to the pion energies obtained before the values of Δ shown in Table II. In this case we subtract 5.7 MeV for the π^0 and 13.4 MeV for the π^- . As a consequence of that, the π^- energy is considerably reduced with respect to the former case and the π^0 energies are also reduced although in a smaller amount. Several consequences appear from the proper consideration of this energy: (a) The π^- width is reduced by a factor of 30. (b) The π^0 width is reduced by about a factor of 3. (c) The effects of the pion renormalization are smaller than before for the π^- and similar for the π^0 case. The enhancement factors due to the pion renormalization are now a factor 20 for π^- and a factor of 7 for the π^0 . The

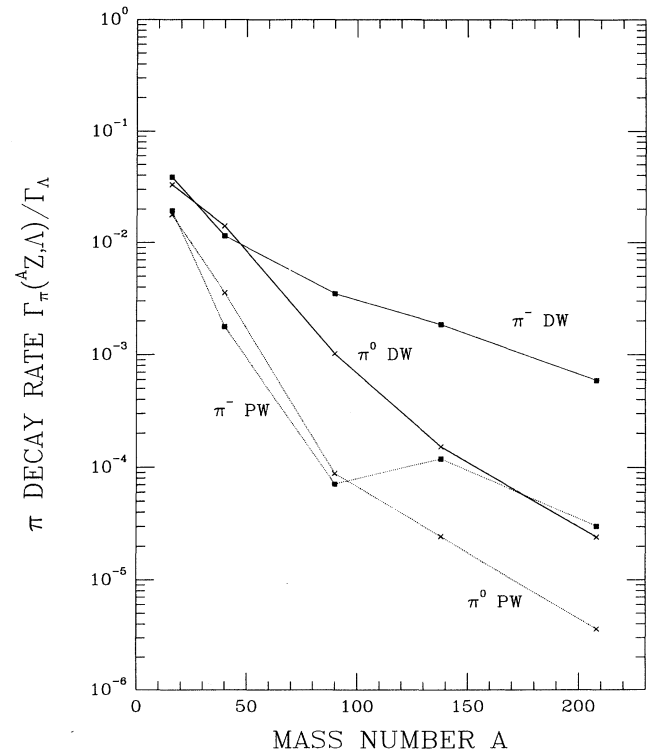


FIG. 3. Pionic decay rate for π^0 and π^- as a function of the mass number (of the host nucleus, ^{16}O , ^{40}Ca , ^{90}Zr , ^{138}Ba , and ^{208}Pb). The dotted lines show the calculations with plane waves for the pion and the solid lines the results with pion distorted waves.

TABLE III. Contribution to the mesonic width of $^{209}_{\Lambda}\text{Pb}$ [units: $\Gamma_{\text{free}}^{\text{total}}$, Eq. (4)] from each of the nuclear levels and the continuum. We show the results for π^-p and π^0n decay using the strict energies which came from the shell model, (a) for $\Lambda \rightarrow \pi^-p$ decay and (b) for π^0n decay. First column: nuclear and continuum levels of the final state. Second column: F.P. stands for the full optical potential or Ref. [18]. N.Q. it is the optical potential obtained by switching off the imaginary part of the optical potential (F.P.) related to quasielastic pion scattering. Third column: Momentum of the pion from the Λ decay when the nucleon is accommodated in the free level j of the nucleus. Fourth column: Factor $S_j^{(s)} \equiv S_j^{(p)}$ in the P.W. approximation for the outgoing pion. Fifth and sixth columns: Factors $S_j^{(s)}$ and $S_j^{(p)}$ [Eq. (11)]. Seventh column: $R_{\text{P.W.}}$, mesonic width (in units of the free width) in the plane-wave approximation for the outgoing pion. Eighth column: $R'_{\text{D.W.}}$, mesonic width in the approximation of fixed π -momentum (this consists in taking $S_j^{(p)} = S_j^{(s)}$) in units of the free width. Ninth column: $R_{\text{D.W.}}$, mesonic width in units of the free width. If the values obtained with the potential N.Q. are not quoted that means they are the same than those obtained with the potential F.P.

State	Potential	q_j (MeV)	$S_{j(\text{P.W.})}^{(s)}$	$S_j^{(s)}$	$S_j^{(p)}$	$R_{\text{P.W.}}$	$R'_{\text{D.W.}}$	$R_{\text{D.W.}}$
(a) ^{208}Pb , $\Lambda \rightarrow p\pi^-$								
1h	F.P.	87.3	5.8×10^{-5}	2.0×10^{-3}	7.3×10^{-3}	4.0×10^{-5}	1.4×10^{-3}	1.7×10^{-3}
	N.Q.			2.5×10^{-3}	1.1×10^{-2}		1.7×10^{-3}	2.2×10^{-3}
2f	F.P.	79.4	1.4×10^{-6}	8.8×10^{-3}	3.9×10^{-2}	8.2×10^{-7}	5.4×10^{-3}	6.8×10^{-3}
	N.Q.			1.3×10^{-2}	6.1×10^{-2}		7.9×10^{-3}	1.0×10^{-2}
3p	F.P.	75.9	2.5×10^{-4}	4.0×10^{-3}	2.8×10^{-2}	1.5×10^{-4}	2.4×10^{-3}	3.3×10^{-3}
	N.Q.			7.1×10^{-3}	4.1×10^{-2}		4.1×10^{-3}	5.5×10^{-3}
1i	F.P.	72.1	8.5×10^{-7}	1.6×10^{-5}	3.0×10^{-4}	4.7×10^{-7}	9.0×10^{-6}	1.9×10^{-5}
2g	F.P.	62.6	1.4×10^{-6}	2.1×10^{-4}	3.4×10^{-3}	6.6×10^{-7}	9.7×10^{-5}	1.7×10^{-4}
	N.Q.			1.5×10^{-4}	2.6×10^{-3}		7.1×10^{-5}	1.3×10^{-4}
3d	F.P.	58.5	6.9×10^{-6}	4.4×10^{-4}	5.8×10^{-3}	3.0×10^{-6}	1.9×10^{-4}	2.9×10^{-4}
	N.Q.			3.6×10^{-4}	3.9×10^{-3}		1.6×10^{-4}	2.2×10^{-4}
4s	F.P.	57.4	5.8×10^{-6}	1.4×10^{-4}	1.3×10^{-3}	2.5×10^{-6}	6.0×10^{-5}	8.1×10^{-5}
	N.Q.			1.3×10^{-4}	8.2×10^{-4}		5.7×10^{-5}	6.9×10^{-5}
1j	F.P.	52.4	3.7×10^{-10}	2.4×10^{-8}	1.1×10^{-7}	1.4×10^{-10}	9.4×10^{-9}	1.1×10^{-8}
4p	F.P.	44.7	5.9×10^{-6}	2.6×10^{-5}	1.8×10^{-4}	1.9×10^{-6}	8.5×10^{-6}	9.8×10^{-6}
Sum	F.P.					2.0×10^{-4}	9.6×10^{-3}	1.2×10^{-2}
	N.Q.						1.4×10^{-2}	1.8×10^{-2}
(b) ^{208}Pb , $\Lambda \rightarrow n\pi^0$								
1i	F.P.	80.3	1.3×10^{-6}	1.3×10^{-6}	1.0×10^{-5}	4.1×10^{-7}	4.1×10^{-7}	6.2×10^{-7}
	N.Q.			1.5×10^{-5}	3.1×10^{-4}		6.6×10^{-7}	4.1×10^{-6}
2g	F.P.	71.9	2.4×10^{-6}	1.2×10^{-5}	2.8×10^{-4}	6.6×10^{-7}	3.4×10^{-6}	7.9×10^{-6}
	N.Q.			1.0×10^{-4}	8.7×10^{-4}		2.7×10^{-5}	4.0×10^{-5}
3d	F.P.	68.5	1.8×10^{-5}	1.0×10^{-4}	9.7×10^{-4}	4.6×10^{-6}	2.6×10^{-5}	3.8×10^{-5}
	N.Q.			1.0×10^{-4}	8.7×10^{-4}		2.6×10^{-5}	3.8×10^{-5}
4s	F.P.	67.5	1.1×10^{-5}	3.4×10^{-5}	3.8×10^{-4}	2.8×10^{-6}	9.7×10^{-6}	1.4×10^{-5}
	N.Q.			3.7×10^{-5}	3.4×10^{-4}		9.4×10^{-6}	1.4×10^{-5}
1j	F.P.	63.3	4.7×10^{-9}	4.7×10^{-9}	4.7×10^{-9}	1.1×10^{-9}	1.1×10^{-9}	1.1×10^{-9}
4p	F.P.	57.1	8.2×10^{-6}	7.9×10^{-6}	3.5×10^{-5}	1.8×10^{-6}	1.7×10^{-6}	1.9×10^{-6}
	N.Q.			7.2×10^{-6}	3.1×10^{-5}		1.5×10^{-6}	1.8×10^{-6}
5s	F.P.	55.4	1.6×10^{-7}	1.0×10^{-6}	3.6×10^{-5}	3.2×10^{-8}	2.1×10^{-7}	4.8×10^{-7}
	N.Q.			9.8×10^{-7}	3.5×10^{-5}		2.0×10^{-7}	4.7×10^{-7}
3f	F.P.	54.9	1.3×10^{-8}	1.8×10^{-6}	6.7×10^{-5}	2.8×10^{-9}	3.7×10^{-7}	8.6×10^{-7}
	N.Q.			1.8×10^{-6}	6.2×10^{-5}		3.6×10^{-7}	8.2×10^{-7}
2h	F.P.	54.6	4.4×10^{-8}	4.4×10^{-8}	4.4×10^{-8}	9.0×10^{-9}	9.0×10^{-9}	9.0×10^{-9}
4d	F.P.	54.0	6.8×10^{-7}	8.6×10^{-7}	3.1×10^{-5}	1.4×10^{-7}	1.7×10^{-7}	3.9×10^{-7}
	N.Q.			8.1×10^{-7}	3.0×10^{-5}		1.6×10^{-7}	3.7×10^{-7}
5p	F.P.	50.5	6.2×10^{-6}	1.0×10^{-5}	9.2×10^{-5}	1.2×10^{-6}	1.9×10^{-6}	2.4×10^{-6}
	N.Q.			9.9×10^{-6}	8.7×10^{-5}		1.9×10^{-6}	2.3×10^{-6}
3g	F.P.	50.2	2.2×10^{-10}	2.2×10^{-10}	1.9×10^{-7}	4.1×10^{-11}	4.1×10^{-11}	1.1×10^{-9}
4f	F.P.	49.5	1.9×10^{-9}	6.7×10^{-7}	7.3×10^{-5}	3.4×10^{-10}	1.2×10^{-7}	5.2×10^{-7}
	N.Q.			6.6×10^{-7}	7.0×10^{-5}		1.2×10^{-7}	5.0×10^{-7}
3h	F.P.	46.5	2.5×10^{-10}	2.5×10^{-10}	2.5×10^{-10}	4.2×10^{-11}	4.2×10^{-11}	4.2×10^{-11}
6s	F.P.	44.1	3.9×10^{-6}	7.8×10^{-7}	6.8×10^{-5}	6.4×10^{-7}	1.3×10^{-7}	3.9×10^{-7}
	N.Q.			7.5×10^{-7}	6.8×10^{-5}		1.2×10^{-7}	3.8×10^{-7}
2i	F.P.	43.6	1.0×10^{-11}	1.0×10^{-11}	1.0×10^{-11}	1.6×10^{-12}	1.6×10^{-12}	1.6×10^{-12}
5d	F.P.	42.8	8.5×10^{-7}	6.6×10^{-7}	5.1×10^{-5}	1.3×10^{-7}	1.0×10^{-7}	2.9×10^{-7}
	N.Q.			6.2×10^{-7}	5.1×10^{-5}		9.8×10^{-8}	2.8×10^{-7}
Sum	F.P.					1.2×10^{-5}	4.6×10^{-5}	7.1×10^{-5}
	N.Q.						4.4×10^{-5}	6.7×10^{-5}

remarkable change from a factor of 60 to a factor of 20 in the case of π^- has to be seen again in the appreciable reduction produced in the π^- energy.

(iv) Another consequence of this smaller energy available for the pion is that the effects of eliminating the quasielastic imaginary part of the potential are smaller than before.

(v) With decreased energy for the pion the transition to excited states is more difficult and the contribution from the excited states in the continuum becomes smaller. Indeed in our model in the π^- case it is zero since there is not enough energy to reach the continuum. In the case of the π^0 it is still about 10% as before. Note that we are discretizing the continuum, hence the lowest eigenstate with positive energy has a small but finite value. There can be small variations in what we call transitions to the continuum with respect to a more realistic case. In any case this fraction of the decay is very small, as we see, and the total decay rate is well calculated since we are implementing a realistic complete set of nucleon states.

The same qualitative features can be appreciated for the other nuclei which we have calculated. We do not

show the details but summarize the results in Table V where only the results using the proper energies are shown. A graphical representation of some of the results is shown in Fig. 3. We show in the tables the contribution for several nuclei using free waves or renormalized waves. We also show for the purpose of comparison the results with a fixed π -momentum approximation if the term $\nabla\Phi_\pi(x)$ in Eq. (5) is replaced by $-i\mathbf{q}\Phi_\pi(x)$ and hence $S^{(s)}$ and $S^{(p)}$ are equal.

The results in Table V can be summarized as follows: (i) The π^- widths (in units of the free width) range from 3.8×10^{-2} in ${}^{17}_\Lambda\text{O}$ to 5.9×10^{-4} in ${}^{209}_\Lambda\text{Pb}$. Those of the π^0 range from 3.3×10^{-2} in ${}^{17}_\Lambda\text{O}$ to 2.4×10^{-5} in ${}^{209}_\Lambda\text{Pb}$. (ii) The effect of the pion renormalization is much smaller in light nuclei. In ${}^{17}_\Lambda\text{O}$, it increases the width of the π^- and π^0 in about a factor of 2. (iii) The balance of energies makes the π^0 and π^- decays in ${}^{17}_\Lambda\text{O}$ comparable, in spite of the factor 2 smaller weight from the $\Delta T = \frac{1}{2}$ for the π^0 and the smaller enhancement from the pion renormalization. In ${}^{41}_\Lambda\text{Ca}$ the π^0 width becomes bigger than the one of the π^- . (iv) The use of the fixed π -momentum approx-

TABLE IV. We show the same results as in Table III, however, taking into account the proper experimental energies, as we discussed in Sec. III.

State	Potential	q_j (MeV)	$S_{j(\text{P.W.})}^{(s)}$	$S_j^{(s)}$	$S_j^{(p)}$	$R_{\text{P.W.}}$	$R'_{\text{D.W.}}$	$R_{\text{D.W.}}$
(a) ${}^{208}\text{Pb}$, $\Lambda \rightarrow p\pi^-$								
1h	F.P.	62.6	2.2×10^{-6}	1.5×10^{-4}	8.7×10^{-4}	1.0×10^{-6}	7.1×10^{-5}	8.6×10^{-5}
	N.Q.			1.6×10^{-4}	9.0×10^{-4}		7.4×10^{-5}	9.0×10^{-5}
2f	F.P.	50.3	3.1×10^{-6}	1.1×10^{-3}	7.4×10^{-3}	1.2×10^{-6}	4.0×10^{-4}	4.7×10^{-4}
	N.Q.			7.6×10^{-4}	5.8×10^{-3}		2.8×10^{-4}	3.4×10^{-4}
3p	F.P.	45.0	8.4×10^{-5}	3.9×10^{-4}	1.0×10^{-2}	2.8×10^{-5}	1.3×10^{-4}	2.1×10^{-4}
	N.Q.			2.9×10^{-4}	7.6×10^{-3}		9.7×10^{-5}	1.6×10^{-4}
1i	F.P.	38.8	7.0×10^{-10}	2.0×10^{-7}	2.0×10^{-6}	2.0×10^{-10}	4.0×10^{-8}	5.0×10^{-8}
Sum	F.P.					3.0×10^{-5}	6.0×10^{-4}	7.7×10^{-4}
	N.Q.						4.6×10^{-4}	5.9×10^{-4}
(b) ${}^{208}\text{Pb}$, $\Lambda \rightarrow n\pi^0$								
1i	F.P.	69.4	2.6×10^{-7}	2.6×10^{-7}	2.6×10^{-7}	7.0×10^{-8}	7.0×10^{-8}	7.0×10^{-8}
2g	F.P.	59.8	1.1×10^{-6}	4.0×10^{-6}	1.3×10^{-4}	2.5×10^{-7}	9.0×10^{-7}	2.2×10^{-6}
	N.Q.			3.7×10^{-6}	1.3×10^{-4}		8.3×10^{-7}	2.0×10^{-6}
3d	F.P.	55.7	5.1×10^{-6}	3.2×10^{-5}	8.6×10^{-4}	1.1×10^{-6}	6.6×10^{-6}	1.3×10^{-5}
	N.Q.			3.1×10^{-5}	8.2×10^{-4}		6.4×10^{-6}	1.3×10^{-5}
4s	F.P.	54.6	4.9×10^{-6}	1.8×10^{-5}	4.9×10^{-4}	1.0×10^{-6}	3.7×10^{-6}	7.2×10^{-6}
	N.Q.			1.8×10^{-5}	4.7×10^{-4}		3.6×10^{-6}	6.9×10^{-6}
1j	F.P.	49.5	1.7×10^{-10}	1.7×10^{-10}	1.7×10^{-10}	3.0×10^{-11}	3.0×10^{-11}	3.0×10^{-11}
4p	F.P.	41.6	5.1×10^{-6}	6.0×10^{-6}	4.6×10^{-5}	7.7×10^{-7}	9.1×10^{-7}	1.0×10^{-6}
	N.Q.			5.8×10^{-6}	4.4×10^{-5}		8.9×10^{-7}	1.0×10^{-6}
5s	F.P.	39.4	7.0×10^{-7}	5.4×10^{-7}	6.1×10^{-5}	1.0×10^{-7}	7.7×10^{-8}	2.5×10^{-7}
	N.Q.			5.3×10^{-7}	6.1×10^{-5}		7.7×10^{-8}	2.5×10^{-7}
3f	F.P.	38.7	1.0×10^{-8}	1.0×10^{-8}	5.9×10^{-5}	2.0×10^{-9}	2.0×10^{-9}	1.6×10^{-7}
2h	F.P.	38.3	2.0×10^{-9}	2.0×10^{-9}	2.0×10^{-9}	3.0×10^{-10}	3.0×10^{-10}	3.0×10^{-10}
4d	F.P.	37.4	1.5×10^{-7}	1.1×10^{-7}	4.5×10^{-5}	2.0×10^{-8}	1.6×10^{-8}	1.2×10^{-7}
	N.Q.			1.1×10^{-7}	4.5×10^{-5}		1.5×10^{-8}	1.2×10^{-7}
5p	F.P.	32.4	2.8×10^{-6}	7.4×10^{-6}	2.1×10^{-4}	3.3×10^{-7}	8.8×10^{-7}	1.2×10^{-6}
	N.Q.			7.4×10^{-6}	2.0×10^{-4}		8.7×10^{-7}	1.2×10^{-6}
Sum	F.P.					3.6×10^{-6}	1.3×10^{-5}	2.5×10^{-5}
	N.Q.						1.3×10^{-5}	2.4×10^{-5}

imation, hence using $S^{(p)}=S^{(s)}$, changes the results of the level of 10% in light nuclei and at the level of 30% for π^- or 80% for π^0 in heavy nuclei. These differences can be taken approximately as a contribution from the p -wave part, or parity-conserving part. Indeed, for the free decay the p -wave part contributes about 13% to the width. In the fixed π -momentum approximation $S^{(p)}$ is taken equal to $S^{(s)}$ and, since the pion momentum is now smaller than in the free case, the contribution of the p -

wave part is below 10%. However, when the proper treatment is given, $S^{(p)}$ is much more strongly renormalized than $S^{(s)}$, as can be seen in Tables III and IV. This is because $-iq\Phi_\pi$ is substituted by $\nabla\Phi_\pi$ and the momentum components of the pion wave function inside the nucleus in the presence of an attractive potential are larger than the asymptotic value. Hence, the difference between the results of Eq. (10) and the fixed π -momentum approximation provide practically all the contribution of the p -

TABLE V. Contributions to the mesonic width for several nuclei from nuclear excited levels (upperindex b) and the continuum (upperindex c) using free waves (P.W.) or renormalized waves (D.W.). $R'_{D.W.}$ stands for the fixed π -momentum approximation, discussed in the text and Table IV. The meaning of the potentials F.P. and N.Q. is the same as in Table IV. Units: Free lambda width. (a) Partial contribution from bound states and the continuum. (b) Total decay widths.

(a)							
Hypernu.	Potential	$R_{P.W.}^b$	$R_{P.W.}^c$	$R'_{D.W.}$	$R'_{D.W.}$	$R_{D.W.}^b$	$R_{D.W.}^c$
$^{17}_\Lambda\text{O}$	π^- F.P.	1.84×10^{-2}	9.0×10^{-4}	3.25×10^{-2}	1.9×10^{-3}	3.55×10^{-2}	2.7×10^{-3}
	π^- N.Q.			3.28×10^{-2}	1.8×10^{-3}	3.59×10^{-2}	2.6×10^{-3}
	π^0 F.P.	1.66×10^{-2}	1.2×10^{-3}	2.67×10^{-2}	2.2×10^{-3}	2.88×10^{-2}	3.0×10^{-3}
$^{41}_\Lambda\text{Ca}$	π^0 N.Q.			2.80×10^{-2}	2.2×10^{-3}	3.02×10^{-2}	2.9×10^{-3}
	π^- F.P.	1.39×10^{-3}	3.9×10^{-4}	7.32×10^{-3}	7.1×10^{-4}	1.00×10^{-2}	1.2×10^{-3}
	π^- N.Q.			7.70×10^{-3}	6.6×10^{-4}	1.04×10^{-2}	1.1×10^{-3}
	π^0 F.P.	3.09×10^{-3}	4.7×10^{-4}	8.50×10^{-3}	9.9×10^{-4}	1.13×10^{-2}	1.4×10^{-3}
$^{91}_\Lambda\text{Zr}$	π^0 N.Q.			9.52×10^{-3}	1.0×10^{-3}	1.27×10^{-2}	1.4×10^{-3}
	π^- F.P.	6.10×10^{-5}	1.0×10^{-5}	2.52×10^{-3}	1.1×10^{-4}	3.42×10^{-3}	1.6×10^{-4}
	π^- N.Q.			2.54×10^{-3}	9.0×10^{-5}	3.36×10^{-3}	1.4×10^{-4}
	π^0 F.P.	7.23×10^{-5}	1.6×10^{-5}	7.07×10^{-4}	5.1×10^{-5}	9.78×10^{-4}	7.8×10^{-5}
$^{139}_\Lambda\text{Ba}$	π^0 N.Q.			6.94×10^{-4}	4.8×10^{-5}	9.46×10^{-4}	7.4×10^{-5}
	π^- F.P.	1.19×10^{-4}	0.0	1.78×10^{-3}	0.0	2.23×10^{-3}	0.0
	π^- N.Q.			1.47×10^{-3}	0.0	1.86×10^{-3}	0.0
	π^0 F.P.	1.23×10^{-5}	1.2×10^{-5}	7.78×10^{-5}	1.1×10^{-5}	1.43×10^{-4}	1.9×10^{-5}
$^{209}_\Lambda\text{Pb}$	π^0 N.Q.			7.40×10^{-5}	1.1×10^{-5}	1.35×10^{-4}	1.8×10^{-5}
	π^- F.P.	3.03×10^{-5}	0.0	5.96×10^{-4}	0.0	7.67×10^{-4}	0.0
	π^- N.Q.			4.56×10^{-4}	0.0	5.91×10^{-4}	0.0
	π^0 F.P.	2.38×10^{-6}	1.2×10^{-6}	1.13×10^{-5}	1.9×10^{-6}	2.26×10^{-5}	2.8×10^{-6}
	π^0 N.Q.			1.08×10^{-5}	1.9×10^{-6}	2.16×10^{-5}	2.7×10^{-6}
(b)							
Hypernu.	Potential	$R_{P.W.}^{\text{total}}$	$R'_{D.W.}$	$R_{D.W.}^{\text{total}}$			
$^{17}_\Lambda\text{O}$	π^- F.P.	1.93×10^{-2}	3.44×10^{-2}	3.82×10^{-2}			
	π^- N.Q.		3.46×10^{-2}	3.85×10^{-2}			
	π^0 F.P.	1.78×10^{-2}	2.89×10^{-2}	3.18×10^{-2}			
$^{41}_\Lambda\text{Ca}$	π^0 N.Q.		3.02×10^{-2}	3.31×10^{-2}			
	π^- F.P.	1.78×10^{-3}	8.03×10^{-3}	1.12×10^{-2}			
	π^- N.Q.		8.36×10^{-3}	1.15×10^{-2}			
	π^0 F.P.	3.56×10^{-3}	9.49×10^{-3}	1.27×10^{-2}			
$^{91}_\Lambda\text{Zr}$	π^0 N.Q.		1.05×10^{-2}	1.41×10^{-2}			
	π^- F.P.	7.14×10^{-5}	2.63×10^{-3}	3.58×10^{-3}			
	π^- N.Q.		2.63×10^{-3}	3.50×10^{-3}			
	π^0 F.P.	8.83×10^{-5}	7.58×10^{-4}	1.06×10^{-3}			
$^{139}_\Lambda\text{Ba}$	π^0 N.Q.		7.42×10^{-4}	1.02×10^{-3}			
	π^- F.P.	1.19×10^{-4}	1.78×10^{-3}	2.23×10^{-3}			
	π^- N.Q.		1.47×10^{-3}	1.86×10^{-3}			
	π^0 F.P.	2.45×10^{-5}	8.89×10^{-5}	1.62×10^{-4}			
$^{209}_\Lambda\text{Pb}$	π^0 N.Q.		8.49×10^{-5}	1.53×10^{-4}			
	π^- F.P.	3.03×10^{-5}	5.96×10^{-4}	7.67×10^{-4}			
	π^- N.Q.		4.56×10^{-4}	5.91×10^{-4}			
	π^0 F.P.	3.61×10^{-6}	1.32×10^{-5}	2.54×10^{-5}			
	π^0 N.Q.		1.27×10^{-5}	2.43×10^{-5}			

wave part. (v) The contribution from the continuum is always small in the nuclei of Table V, of the order of 10% or smaller. (vi) The effect of omitting the quasielastic contribution in the optical potential is also rather small once the proper energies are considered.

With respect to the results of Ref. [13] there are some important differences which arise mostly from the proper consideration of the energy balance which we do here. (We have checked that under the same assumptions as in Ref. [13] we get the same results within 30%.) (i) The width of the π^- decay in $^{209}_{\Lambda}\text{Pb}$ is about one order of magnitude smaller than the one in Ref. [13]. The π^0 width is about a factor of 4 smaller. (ii) The widths of π^- and π^0 decay in $^{41}_{\Lambda}\text{Ca}$ are inverted here with respect to Ref. [13]. Here the π^0 width is bigger than the π^- one. In absolute numbers our π^0 width is about 2 times larger than in Ref. [13]. (iii) The π^- decay width as a function of A is a decreasing function in our case, while in Ref. [13] the π^- width increases smoothly from $A \simeq 80$ on.

VI. RESULTS FOR $^{12}_{\Lambda}\text{C}$

This nucleus has been thoroughly investigated in the last years and we deal with it separately in order to compare with the experimental results. In this case we find $M(^{12}\text{N}) - M(^{11}\text{C}) = 938.2$ MeV and $M(^{12}\text{C}) - M(^{11}\text{C}) = 920.9$ MeV. The binding energy of the Λ 1s state is 12.4 MeV. In the shell-model potential with 11 nucleons the 1s, 1p states are bound and the rest appear already in the continuum. The nucleons hence go to the empty states in the 1p shell and then to the continuum. The value of $m_p + E_{1p}$ in the shell model is 929 MeV and of $m_n + E_{1p} = 930.3$. Hence, in the case of π^- decay we must subtract 8.7 MeV from the π^- energy provided by the shell model and add 9.4 MeV to the π^0 energy. This has as a consequence that the π^0 decay is now particularly favored. Because of the larger energies available in the π^0 decay there is also an appreciable contribution from the continuum which is of about 25%, while in the π^- decay this magnitude is much smaller, 5%.

Our results, which we compare with experiment, are the following:

$$\frac{\Gamma_{\pi^0}}{\Gamma_{\Lambda}} = 0.159 \quad (\text{experiment [30] } 0.217 \pm 0.084),$$

$$\frac{\Gamma_{\pi^-}}{\Gamma_{\Lambda}} = 0.086 \quad (\text{experiment [5] } 0.052^{+0.063}_{-0.035}),$$

$$\frac{\Gamma_{\pi^0}}{\Gamma_{\pi^-}} = 1.86,$$

The agreement with experiment is good although the experimental errors are still large. In Ref. [13] the follow-

ing results are obtained $\Gamma_{\pi^0}/\Gamma_{\Lambda} = 0.130$, $\Gamma_{\pi^-}/\Gamma_{\Lambda} = 0.098$, $\Gamma_{\pi^0}/\Gamma_{\pi^-} = 1.32$. Thus our results are larger than those of Ref. [13] for the π^0 decay and smaller for the π^- decay. The ratio of π^0/π^- decay is about 40% larger in our case. The experimental errors are, however, still too large to draw any conclusions from these differences.

VII. CONCLUSIONS

We have analyzed the problem of mesonic lambda decay in medium and heavy nuclei, by considering shell-model wave functions for the nucleons and proper wave functions for the pions in the medium. As novelties with respect to former work we have introduced the following points.

(i) We have calculated the strength for decay into continuum states, apart for the decay into excited bound states. We found it to be generally a small fraction of the total, of the order of 10% or less. In some particular cases the correction is more relevant, like in the case of the π^0 decay of $^{12}_{\Lambda}\text{C}$ where the proportion of decay to the continuum was about 25%.

(ii) We have also used a pion nucleus optical potential which allows the separation of its imaginary part into a piece related to the quasielastic scattering of pions and another piece related to pion absorption. We removed the quasielastic part in order not to eliminate from the pion flux the pions which undergo quasielastic collisions. This led to increases of 50% in the π^- width of $^{209}_{\Lambda}\text{Pb}$ when the shell-model energies were used, and smaller changes in other cases. However, when more accurate energies taken from experiment were used, these effects became smaller, of the order of 10% or below.

(iii) We looked into detail for the energy balance of the reaction by taking the energies from the experimental masses of the nuclei involved rather than those coming from the nucleon shell model. This was very important and led to a reduction by a factor of 30 of the π^- decay in $^{209}_{\Lambda}\text{Pb}$ with respect to the expectations of the shell model, and about a factor of three reduction for the π^0 decay. Similar or smaller modifications were found in other nuclei. This energy balance had as a consequence the relative enhancement of π^0 decay with respect to π^- decay, and in nuclei like $^{41}_{\Lambda}\text{Ca}$ the π^0 decay rate was bigger than that of the π^- . In $^{12}_{\Lambda}\text{C}$ it also led to an appreciable enhancement of the π^0 width, with respect to π^- , which follows closely the experimental trend.

With respect to former calculations [13] the results obtained here introduce important corrections, among them the following. (i) The width for π^- decay of $^{209}_{\Lambda}\text{Pb}$ is one order of magnitude smaller in our approach. (ii) The π^0 and π^- decay widths are inverted in $^{41}_{\Lambda}\text{Ca}$: We obtain a larger fraction of π^0 than π^- decay. (iii) We find a decrease of the π^- width as A increases, opposite to the results of Ref. [13] which show a moderate increase from $A \simeq 80$. (iv) In $^{12}_{\Lambda}\text{C}$ we find a larger π^0 width and a smaller π^- width. As a consequence the ratio $\Gamma_{\pi^0}/\Gamma_{\pi^-}$ is about 40% larger in our case than in Ref. [13]. On the

other hand, we find again, as had been shown before qualitatively in Ref. [10] and more quantitatively in Refs. [11–13], the important role of the pion renormalization in the medium, which produces large enhancements of the mesonic widths with respect to the plane wave results, particularly in heavy nuclei.

ACKNOWLEDGMENTS

This work is supported in part from the Spanish CICYT Contract No. AEN 90-0049. J. Nieves wishes to acknowledge the financial support from Ministerio de Educacion y Ciencia.

-
- [1] A. Montwill *et al.*, Nucl. Phys. **A234**, 413 (1974).
 - [2] R. Grace *et al.*, Phys. Rev. Lett. **55**, 1055 (1985).
 - [3] A. Sakaguchi *et al.*, Nuovo Cimento **102A**, 511 (1989).
 - [4] P. D. Barnes, Nucl. Phys. **A450**, 43c (1986); **A478**, 127c (1988).
 - [5] J. J. Szymanski *et al.*, Phys. Rev. C **43**, 849 (1991).
 - [6] R. H. Dalitz, Phys. Rev. **112**, 605 (1958).
 - [7] R. H. Dalitz and L. Liu, Phys. Rev. **116**, 1312 (1959).
 - [8] Y. Kurihara, Y. Akaishi, and H. Tanaka, Phys. Rev. C **31**, 971 (1985).
 - [9] H. Bando and H. Takaki, Prog. Theor. Phys. **72**, 106 (1984); H. Bando, T. Motoba, and J. Zofka, Int. J. Mod. Phys. A **5**, 4021 (1990).
 - [10] E. Oset and L. L. Salcedo, Nucl. Phys. **A443**, 704 (1985).
 - [11] K. Itonaga, T. Motoba, and H. Bando, Z. Phys. A **330**, 209 (1988).
 - [12] T. Motoba, K. Itonaga, and H. Bando, Nucl. Phys. **A489**, 683 (1988).
 - [13] T. Motoba, Nucl. Phys. **A527**, 485c (1991); Few Body Systems, Suppl. **5**, 386 (1992); Proceedings of the International Symposium on Hypernuclear and Strange Particle Physics, Shimoda, 1991 [Nucl. Phys. **A547**, 115c (1992)].
 - [14] E. Oset and L. L. Salcedo, Nucl. Phys. **A450**, 371c (1986).
 - [15] C. B. Dover and G. E. Walker, Phys. Rep. **89**, 1 (1982) and references therein.
 - [16] E. Oset, P. Fernandez de Cordoba, L. L. Salcedo, and R. Brockmann, Phys. Rep. **188**, 79 (1990).
 - [17] J. Nieves, E. Oset, and C. Garcia-Recio, Nucl. Phys. A (in press).
 - [18] J. Nieves, E. Oset, and C. Garcia-Recio, Nucl. Phys. A (in press); C. Garcia-Recio, talk at the *International Workshop on Pions in Nuclei*, Peñiscola, 1991, edited by E. Oset, M. J. Vicente-Vacas, and C. Garcia-Recio (World Scientific, Singapore, 1992), p. 320.
 - [19] B. H. J. McKellar and B. F. Gibson, Phys. Rev. C **30**, 322 (1984).
 - [20] A. Galindo and P. Pascual, *Quantum Mechanics* (Springer, New York, 1991).
 - [21] R. E. Chrien, Nucl. Phys. **A478**, 705c (1988).
 - [22] R. Hausmann and W. Weise, Nucl. Phys. **A491**, 598 (1989).
 - [23] A. Bouyssy, Nucl. Phys. **A290**, 324 (1977); Phys. Lett. **84B**, 41 (1979).
 - [24] P. E. Hodgson, *Nuclear Reactions and Nuclear Structure* (Oxford University Press, Oxford, England, 1971).
 - [25] C. M. Lederer and V. S. Shirley, *Table of Isotopes* (Wiley Interscience, New York, 1978).
 - [26] R. Guardiola and J. Ros, Comp. Phys. **45**, 374 (1982); **45**, 390 (1982).
 - [27] M. Ericson and T. E. O. Ericson, Ann. Phys. (N.Y.) **36**, 323 (1966).
 - [28] R. Seki and K. Masutani, Phys. Rev. C **27**, 2799 (1983).
 - [29] R. Seki, in *Pion-Nucleus Physics: Future Directions and New Facilities at LAMPF*, edited by R. J. Peterson and D. D. Strottman, AIP Conf. Proc. No. 163 (AIP, New York, 1987).
 - [30] A. Sakaguchi *et al.*, Phys. Rev. C **43**, 73 (1991).